Impact of nanosized additives on the fatigue damage behaviour of asphalt mixtures

Impact of nano-sized additives on the fatigue damage behaviour of asphalt mixtures

Journal:	*Fatigue & Fracture of Engineering Materials & Structures*
Manuscript ID	FFEMS-8199
Manuscript Type:	Original Contribution
Date Submitted by the Author:	13-May-2019
Complete List of Authors:	SANTAGATA, Ezio; Politecnico di Torino, DIATI Baglieri, Orazio; Politecnico di Torino, DIATI Miglietta, Fabrizio; Politecnico di Torino, DIATI Tsantilis, Lucia; Politecnico di Torino, DIATI Riviera, Pier Paolo; Politecnico di Torino, DIATI

Impact of nano-sized additives on the fatigue damage behaviour of asphalt mixtures

Ezio Santagata, Orazio Baglieri, Fabrizio Miglietta, Lucia Tsantilis, Pier Paolo Riviera

Abstract: The study presented in this paper aimed at evaluating the impact of different nano-sized additives, including an organophilic nanoclay and multiwall carbon nanotubes, on the fatigue properties of dense-graded asphalt mixtures. Cyclic direct tension fatigue tests were carried out and the corresponding results were interpreted by means of a simplified version of the Visco-Elastic Continuum Damage model. The experimental investigation also included linear viscoelastic characterization of the considered materials. Results derived from tests carried out on the mixtures containing nano-sized additives were compared to those obtained for a reference standard mixture. It was found that the use of the innovative additives can give a substantial contribution to the enhancement of the fatigue damage resistance of asphalt mixtures. Moreover, when comparing the two types of additives, it was observed that organophilic nanoclays can outperform multiwall carbon nanotubes.

Keywords: asphalt mixtures; nanoclays; multiwall carbon nanotubes; linear viscoelastic behaviour; fatigue damage.

$a(T)$	Shift Factor
α	Damage Evolution Rate
β	Load Form Factor
C	Pseudo Secant Modulus
C_f	Pseudo Secant Modulus to Failure
C_{11}, C_{12}	Regression Coefficients
γ	Regression Coefficient
DMR	Dynamic Modulus Ratio
ΔC_j	Change in the Pseudo Secant Modulus
$\Delta\xi$	Change in the Reduced Time
$\Delta\xi_P$	Change in the Reduced Pulse Time
ΔS_i	Change in the Damage
δ	Regression Coefficient
E_a	Activation Energy

$\|E^*\|$	Dynamic Modulus
$\|E^*\|_{LVE}$	Linear Viscoelastic Dynamic Modulus
$E(t)$	Uniaxial Relaxation Modulus
E_R	Reference Modulus
ε^R	Pseudo Strain
ε_{ta}^R	Tension Amplitude Pseudo Strain
$\varepsilon_{0,pp}$	Peak-to-Peak Strain
f_R	Reduced Frequency
k_1, k_2	Regression Coefficients
K_1	Loading Shape Factor
κ	Regression Coefficient
μ	Regression Coefficient
$N_{failure}$ (N_f)	Loading Cycles to Failure
ξ	Reduced Time
ξ_P	Reduced Pulse Time
S	State Variable representing Damage
$S_{initial\ cycle}$	Damage occurring at the first cycle
$S_{failure}$ (S_f)	Damage to Failure
σ	Shear Stress
t	Time of Interest
T	Testing Temperature
T_r	Reference Temperature
τ	Integration Variable
W^R	Pseudo Strain Energy Density

Introduction

In recent years, the possible exploitation of nanotechnologies in the construction of asphalt pavements has been investigated by researchers worldwide in order to improve performance in the presence of increasingly severe environmental and traffic loading conditions.[1]

In such a context, various nano-sized additives have been considered as potential alternatives to traditional bitumen modifiers.[2] As a result of performed investigations, nanoclays and carbon nanotubes have been identified as the most promising products of

this category. In particular, it has been shown that they are capable of improving mechanical properties and durability of asphalt mixtures.[3]

Nanoclays are constituted by thin silicate layers that are arranged to form a final structure which can significantly expand when polar molecules permeate the space between silicate sheets. This peculiar characteristic, along with the high surface-to-volume ratio (referred to as "aspect ratio"), makes nanoclays suitable to be adopted as reinforcing additives.[4] However, since the hydrophilic character of nanoclays impairs their miscibility with any organic polymer, prior to use inorganic exchange cations need to be replaced with a surfactant which provides the nanoparticles with a hydrophobic character.

Carbon nanotubes have a structure formed by graphene sheets which are rolled up into cylindrical elements, thereby leading to configurations that can be either of the singlewall or multiwall type.[5] The aspect ratio of these nano-sized materials is comparable to and even higher than that of nanoclays. The quasi-one-dimensional sp^2-bonded arrangement of nanotubes is mostly responsible for their exceptional mechanical properties. In particular, they exhibit very high values of tensile strength and Young's modulus, and for this reason they can be employed to create composite materials with superior performance.[6]

The overall characteristics of compounds obtained from the combination of nano-sized additives and a base dispersing medium are strongly affected by the interactions taking place between these two components. Carbon nanotubes form different hierarchical morphologies of bundles as a result of entanglement and agglomeration phenomena. In the case of nanoclays, interactions with the dispersing medium may result in intercalated or exfoliated structures. Intercalated structures are organized in a multi-layered system of silicate sheets alternating with polymeric layers, while exfoliated structures consist in well separated platelets.[7,8]

The effectiveness of both nanoclays and carbon nanotubes as reinforcing agents in asphalt binders and mastics has been assessed by many authors. In particular, it has been shown that these types of nano-sized additives, if properly dosed and mixed with the base binder, may have a significant impact on viscoelastic properties, on the resistance to permanent deformation and on fatigue behaviour.[9,10,11,12,13,14,15,16,17]

Few studies have focused on the effects of nanoclays and carbon nanotubes on the performance-related characteristics of asphalt mixtures.

Van de Ven et al.[18] considered the addition of 6 % cloisite to a reference mixture and consequently documented an enhancement of stiffness, tensile strength and rutting resistance. However, they found that the modified mixture exhibited worse fatigue damage properties than the reference one. By contrast, an increase of endurable damage was reported by Miglietta et al.[19] for asphalt mixtures containing 3 % nanoclay. The same nanoclay percentage was employed by de Melo et al.[20] and also in this case significant improvements in fatigue life were observed, together with non-negligible changes in stiffness and resistance to permanent deformation.

Ameri et al.[21] and Arabani and Faramarzi[22] investigated the use of carbon nanotubes at various dosages, ranging between 0.1 % and 1.5 % by weight of base bitumen. They showed that the increase of carbon nanotubes content led to an increase of dynamic moduli measured in the linear viscoelastic range and to enhanced fatigue resistance properties. Similar results were obtained by de Melo et al.[23]

Further investigations are certainly needed in order to better understand the influence of nano-sized additives on the properties of asphalt mixtures and to foster the use of such innovative materials in road paving applications. To this regard, comparatives studies may be useful to highlight any similarities or differences between various nano-modifiers. In the experimental work presented in this paper, the performance-related properties of asphalt mixtures modified with nanoclay and carbon nanotubes were investigated and compared, with a specific emphasis placed on their fatigue damage behaviour.

Materials and methods

Asphalt mixtures were prepared by using a neat bitumen (B) and two nano-modified asphalt binders (NB and CB). These were obtained by combining bitumen B with an organophilic nanoclay and multiwall carbon nanotubes, respectively.

Bitumen B was subjected to preliminary characterization which included chemical, empirical and rheological tests.

Chemical characterization was conducted by means of a Thin Layer Chromatography (TLC) technique which allows the determination of the relative amounts of saturates, aromatics, resins and asphaltenes (SARA analysis). The procedure adopted for testing, which relies upon the use of a Flame Ionization Detection (FID) device, is similar to that followed in previous studies.[24] Obtained results are displayed in Figure 1 in the form of a chromatogram, in which the voltage variation (ΔV) recorded by the FID system is plotted as a function of time. Percentages of bitumen fractions are

consequently calculated as the integrals of the represented peaks. As indicated in Figure 1, it was found that bitumen B possessed a relative high quantity of aromatics (65.3 %), thus suggesting that it may be a binder which can activate significant interactions with nano-sized additives, with parts of its oily fraction possibly seeping through the nanotubes and layered silicate structures.

Empirical characterization included the determination of penetration at 25 °C (according to EN 1426) and ring and ball softening point (according to EN 1427). Recorded values of these parameters are reported in Table 1 (left hand side). Although not all tests necessary for characterization according to EN 12591 were performed, bitumen B exhibited properties which are those of a 70/100 penetration grade binder.

Rheological characterization was carried out with the purpose of determining the Performance Grade (PG) of the asphalt binder according to AASHTO M320-10. Results reported in Table 1 (right hand side) show that bitumen B was classified as a PG 58-22 binder. Such an outcome should be simply considered as a reference, since no PG grading was carried out on nano-modified binders NB and CB.

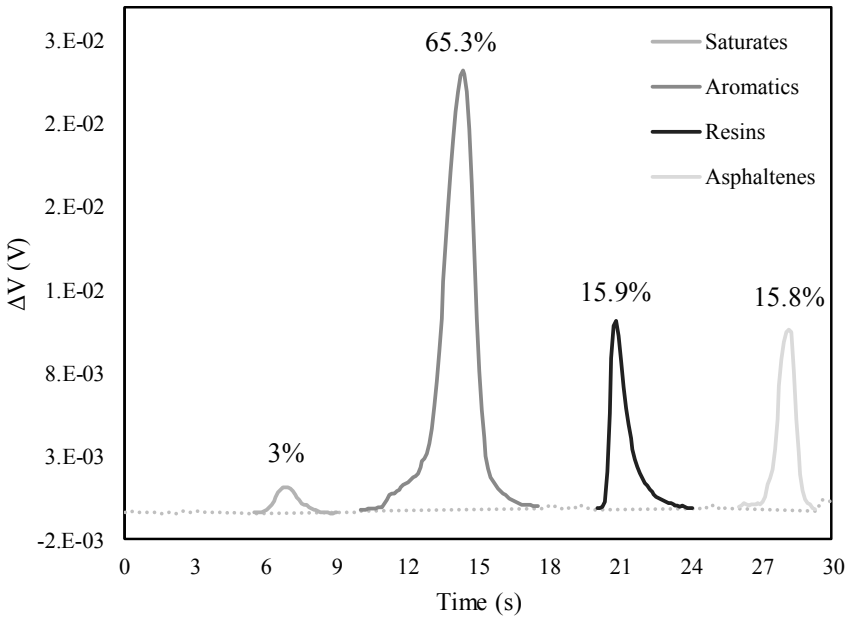

Fig. 1. Chromatogram of neat bitumen B

Table 1. Results of preliminary characterization tests performed on neat bitumen B

Empirical characterization	Rheological characterization

		Ageing condition	PG parameters	Measured values
Penetration at 25 °C (dmm)	95	Original	T = 135 °C G*/sinδ = 1 kPa	η = 0.347 Pa·s T = 63.3 °C
R&B Softening point (°C)	44.6	RTFOT	G*/sinδ = 2.2 kPa G*·sinδ = 5000 kPa	T = 63.8 °C T = 22.0 °C
		PAV	m = 0.300 S = 300 MPa	T = -14.3 °C T = -16.2 °C

RTFO: Rolling Thin Film Oven; PAV: Pressure Ageing Vessel; η: dynamic viscosity (Brookfield viscometer); T: test temperature; |G*| and δ: norm and phase angle of the complex modulus (Dynamic Shear Rheometer); m and S: creep rate and creep stiffness (Bending Beam Rheometer).

The nano-sized additives used for the preparation of modified asphalt binders were commercially available products. The organophilic nanoclay was originated from natural montmorillonites modified by means of a quaternary ammonium salt used as surfactant coating. Multiwall carbon nanotubes were produced by means of the catalysed chemical vapour deposition technique. Main characteristics of the additives, based on manufacturers' technical specifications, are reported in Table 2 and Table 3.

Table 2. Physical characteristics of the employed nanoclay

Surfactant	Anion	Density [g/cm^3]	Basal spacing [nm]
Dimethyl, dihydrogenatedtallow, quaternary ammonium	Chloride	1.66	3.15

Table 3. Physical characteristics of the employed multiwall carbon nanotubes

Average diameter [nm]	Average length [μm]	Surface area [cm^2 /g]	Carbon purity [%]	Density [g/cm^3]
9.5	1.5	250-300	90	1.72

Blends obtained by adding the nano-sized additives to base binder B were prepared in the laboratory by adopting a three-step procedure. This consists of an initial hand-mixing of the nanoparticles within the previously preheated bitumen, of a subsequent shear mixing phase carried out for 90 minutes at 1550 rpm mixing speed, and of a final sonication phase in which the blends are subjected to ultrasonic waves, of 157.5 μm amplitude for 60 min, applied by means of an ultrasonic homogenizer. The entire preparation process was carried out at a constant temperature of 150 °C. Based on the results of an optimization process conducted in previous studies[12,25], nano-additive percentages (by weight of base binder) were selected equal to 3 % for the nanoclay and to 0.5 % for carbon nanotubes.

The neat and nano-modified binders were combined with selected siliceous aggregates for the preparation of three asphalt mixtures characterized by the same aggregate gradation (Table 4) and by the same target binder content, set equal to 4.8 % by weight of dry aggregates. Such a composition is representative of typical dense-graded mixtures employed for the formation of pavement intermediate courses.

Table 4. Aggregate gradation adopted for asphalt mixtures

Sieve [mm] EN	Passing [%]
16	100
14	91.8
12.5	85.7
10	75.9
8	65.7
6.3	54.4
4	44.7

2	34.0
1	23.1
0.5	15.9
0.25	11.3
0.125	8.3
0.075	6.4

The three asphalt mixtures are hereinafter termed M-B, M-CB and M-NB to identify the type of binder used for their preparation (neat bitumen for M-B, and binder containing nanoclays and carbon nanotubes for M-NB and M-CB, respectively). The unmodified M-B mixture was assumed as a reference in the analysis of test results. Mechanical characterization of asphalt mixtures included the evaluation of linear viscoelastic properties and the assessment of fatigue damage behaviour.

Viscoelastic properties were determined by means of dynamic modulus tests, performed at three temperatures (4, 20 and 35 °C) and multiple loading frequencies (25, 20, 10, 5, 2, 1, 0.5, 0.2, 0.1 and 0.01 Hz) according to AASHTO PP 61-13. Fatigue damage behaviour was assessed by means of cyclic direct tension tests carried out at 15 °C. Such a temperature was selected since it corresponds to the average of the two PG limiting temperatures (minus 3 °C) of neat bitumen B. Tests were run in the strain-controlled mode, with strain levels selected in the 100-300 μm range as per AASHTO TP 107-14.

Dynamic modulus and fatigue tests were carried out by making use of the Asphalt Mixture Performance Tester (AMPT). Cylindrical specimens of 100 mm diameter and 150 mm height were obtained from larger samples of 150 mm diameter and 170 mm height compacted with the gyratory shear compactor. Compaction temperatures were set equal to 140 °C, 155 °C and 170 °C for mixtures M-B, M-CB and M-NB, respectively, in order to take into account the different viscosities of the binders considered in the investigation. Gyratory samples were reduced to testing geometry by extracting cores from their centre and thereafter by trimming the core ends in order to obtain smooth and parallel surfaces. Target air void content was fixed at 4 ± 0.5% for all mixtures. The actual air void content of each specimen was checked prior to

mechanical testing, as per EN 12697-8, by making use of the saturated-surface dry specific gravity.

Linear viscoelastic properties

The overall rheological behaviour of the asphalt mixtures was evaluated by referring to dynamic modulus master curves, which allow the assessment of the mechanical response of viscoelastic materials in a broad range of frequencies.[26] Based on the time-temperature equivalency principle, results of dynamic modulus tests obtained at various temperatures were shifted to the reference temperature of 20 °C. For such a purpose, raw data were fitted to a sigmoidal function, used to mathematically describe the evolution of the dynamic modulus in the frequency domain, and by simultaneously fitting shift factors to the Arrhenius equation, used to model temperature dependency.

The Arrhenius and sigmoidal functions are reported in Equations 1 and 2, respectively:

$$\log a(T) = \frac{E_a}{19.14714}\left(\frac{1}{T} - \frac{1}{T_r}\right) \quad (1)$$

$$\log |E^*| = \kappa + \frac{\mu - \kappa}{1 + e^{\gamma + \delta \log f_R}} \quad (2)$$

where a(T) is the shift factor at the generic test temperature T (K); E_a is a fitting parameter that physically represents activation energy (J/mol); T_r is the reference temperature (K); |E*| is the dynamic modulus (MPa); γ, δ, κ and μ are regression coefficients; f_R is reduced frequency (Hz), calculated as the product of physical frequency f and shift factor a(T).

Fitting coefficients obtained from non-linear regression analyses carried out on experimental data obtained for the three asphalt mixtures are listed in Table 5.

Table 5. Fitting coefficients of the Arrhenius and sigmoidal functions of asphalt mixtures

Mixture	E_a	κ	μ	γ	δ
M-B	184,375	1.693	4.412	-0.856	-0.759
M-NB	183,480	1.692	4.476	-0.911	-0.735
M-CB	188,346	1.703	4.430	-0.943	-0.731

As proven by the similar values of the E_a parameter calculated for the three mixtures, both the nanoclay and the carbon nanotubes did not significantly affect the temperature dependency of the asphalt mixtures. Such an outcome suggests that the two additives did not interfere with the relaxation phenomena which take place in the bituminous matrix. This is probably due to the relatively low additive dosages selected for the preparation of the modified blends as well as to the thermally inert nature of the additives in the range of investigated temperatures.

As indicated by the values of parameters γ, δ, κ and μ, the presence of nano-particles had some effects, although not of remarkable extent, on the dynamic modulus master curve. By referring to the values of κ, which corresponds to the lower asymptote of the sigmoidal equation, a limited increase in the low frequency dynamic modulus was found only when carbon nanotubes were used for modification. On the other hand, the modulus value associated to the upper asymptote of the sigmoidal function, defined by the μ parameter, was slightly higher for materials containing both carbon nanotubes and nanoclays. The effects of nano-sized additives in the linear viscoelastic domain were more evident when considering the shape of the sigmoidal function, both in terms of the position (γ parameter) and slope (δ parameter) of the master curve at its inflection point, with greater changes obtained by employing carbon nanotubes.

The outcomes discussed above are presented in graphical form in Figure 2, where dynamic modulus master curves at 20 °C are displayed in the range of reduced frequencies covered by the shifting of the experimental data.

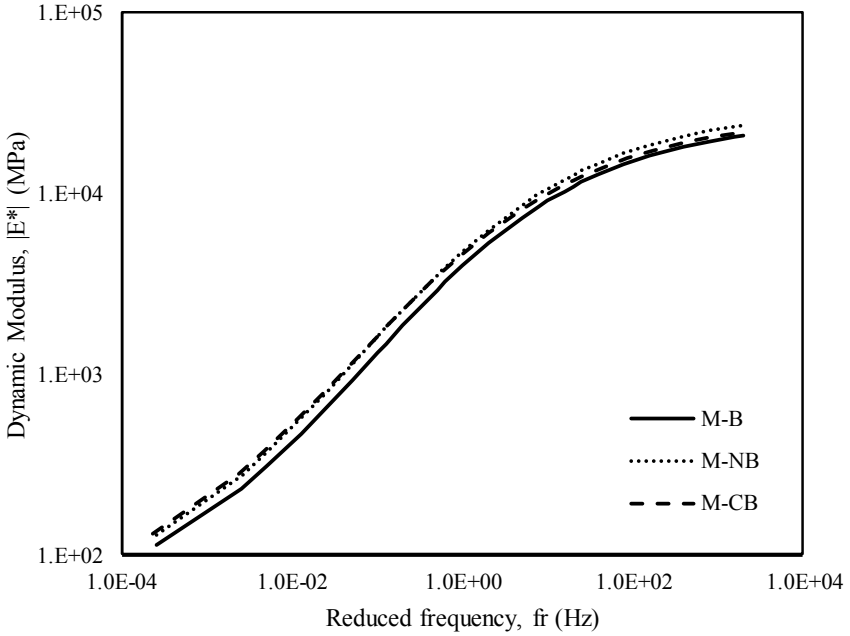

Fig. 2. Dynamic modulus master curves at 20 °C of asphalt mixtures

Fatigue damage behaviour

Processing of raw data obtained from cyclic direct tension fatigue tests was carried out by employing the viscoelastic continuum damage (VECD) approach, the core of which is the identification of a material-dependent constitutive relationship referred to as damage characteristic curve (DCC). The DCC expresses the evolution of the pseudo secant modulus C (chosen as material integrity parameter) as a function of cumulative damage S (which is an internal state variable). This type of representation is fundamental for the characterization of fatigue behaviour since it highlights the intrinsic properties of materials, not being dependent upon temperature, loading mode (i.e. strain- or stress-controlled) and loading type (i.e. cyclic or monotonic).[27,28] Moreover, it allows true fatigue behaviour to be assessed while limiting the effects of other phenomena occurring during time sweep tests.[29]

The model adopted in the VECD framework is based on linear viscoelasticity and continuum damage mechanics concepts, combining Shapery's work potential theory, the elastic-viscoelastic correspondence principle and the time-temperature superposition or equivalency principle.[30,31]

Schapery's work potential theory[32] quantifies damage growth in viscoelastic materials by considering the rate of change in time of a state variable S. Thus, time-dependent changes within the material microstructure are expressed by the following damage evolution law:

$$\frac{dS}{dt} = \left(-\frac{\partial W^R}{\partial S} \right)^{\alpha} \tag{4}$$

where W^R is the pseudo strain energy density and α is the material-dependent damage evolution rate.

In order to derive the S value as a function of time, Equation 4 is solved after substituting W^R with the following expression[33]:

$$W^R = \frac{1}{2} \cdot \sigma \cdot \varepsilon^R = \frac{1}{2} \cdot (\varepsilon^R)^2 \cdot C(S) \tag{5}$$

where σ is applied stress, ε^R is pseudo strain and C is the pseudo secant modulus.

Pseudo strains can be expressed in the convolution form indicated in Equation 6, which stems from the application of the elastic-viscoelastic correspondence principle. The consequence of such an approach is that the inherent viscoelastic problem can be solved by adopting an elastic solution in which physical strains are replaced by pseudo strains.[34] Thus, the pseudo secant modulus C, defined as indicated in Equation 7, benefits from the time-independency of pseudo strains:

$$\varepsilon^R = \frac{1}{E_R} \int_0^t E(t-\tau) \frac{d\varepsilon}{d\tau} d\tau \tag{6}$$

$$C = \frac{\sigma}{\varepsilon^R \cdot DMR} \tag{7}$$

where E(t) is the uniaxial relaxation modulus, E_R is the reference modulus (arbitrarily assumed equal to 1) and DMR is a factor taking into account specimen-to-specimen variability. Material integrity is equal to 1 for the material in its original undamaged state (when S is equal to 0) and decreases monotonically with growing damage.

Adoption of the VECD model in its full formulation requires the entire loading time history of a fatigue test to be precisely tracked and subjected to analysis, thus leading to a cumbersome calculation process. However, a simplified version of the model (the so-called S-VECD) can also be employed with significant benefits in terms of calculation speed and effectiveness. As widely discussed in the literature[31,35], this simplified version can be applied to all loading cycles with the exception of the first one, which needs to be analysed in more detail by means of the complete VECD model.

By following the simplified approach, the cumulative damage of the material is computed by means of Equation 8, in which it is shown that the material state variable representing damage is given by the sum of the damage occurred in the initial loading cycle ($S_{initial\ cycle}$), calculated by applying the rigorous VECD model (Equation 9a), and the incremental damage contribution associated to all the other cycles (ΔS_i), determined by referring to the S-VECD model (Equation 9b).

$$S = S_{initial\ cycle} + \sum_{i=1}^{N} \Delta S_i \tag{8}$$

$$S_{initial\ cycle} = \left(-\frac{DMR}{2} \cdot (\varepsilon^R)_j^{\,2} \cdot \Delta C_j \right)^{\frac{\alpha}{1+\alpha}} \cdot (\Delta\xi)_j^{\frac{1}{1+\alpha}} \qquad \xi \le \xi_P \tag{9a}$$

$$\Delta S_i = \left(-\frac{DMR}{2} \cdot (\varepsilon_{ta}^R)_i^{\,2} \cdot \Delta C_i \right)^{\frac{\alpha}{1+\alpha}} \cdot (\Delta\xi_P)_i^{\frac{1}{1+\alpha}} \cdot (K_1)^{\frac{1}{1+\alpha}} \qquad \xi > \xi_P \tag{9b}$$

where α is a continuum damage power term, ΔC is the change in the pseudo secant modulus, $\Delta\xi$ and $\Delta\xi_P$ are the changes in the reduced time and reduced pulse time, respectively, ε^R and $\varepsilon_{ta}{}^R$ are the peak-to-peak pseudo strain and tension amplitude pseudo strain, respectively, and K_1 is the loading shape factor.

DCCs of the asphalt mixtures were built by fitting C-S data obtained by means of continuum damage modelling to the following power law function (Equation 10)[36,37]:

$$C = 1 - C_{11} \cdot S^{C_{12}} \tag{10}$$

where C_{11} and C_{12} are material-dependent fitting coefficients.

Obtained results are shown in Figure 3, where data have been plotted up to the failure point recorded for each mixture. Failure points were identified at the loading cycles at which a phase angle drop occurred, thus revealing the formation of macro-cracks in the bituminous matrix.[38] Fitting parameters (C_{11} and C_{12}) and C and S values recorded at failure (indicated as C_f and S_f) are listed in Table 6.

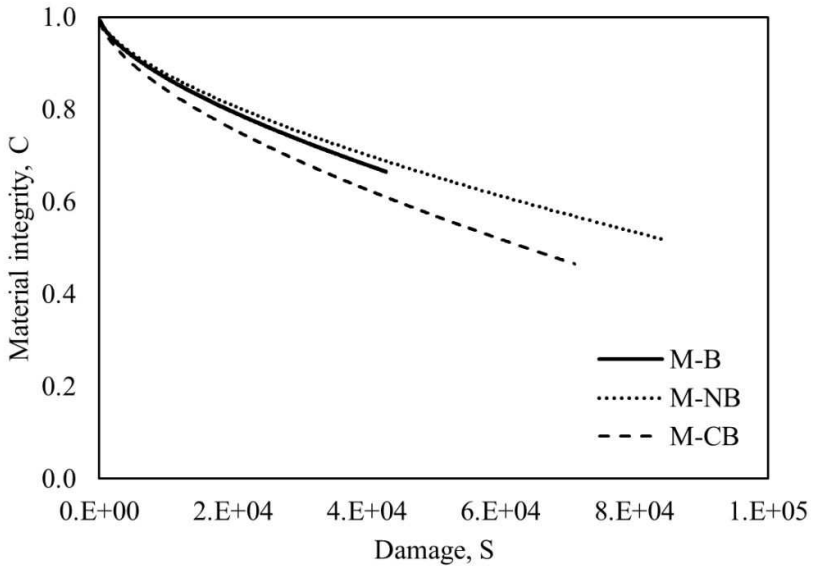

Fig. 3. Damage characteristic curves of asphalt mixtures

Table 6. DCC fitting parameters and C-S values at failure of asphalt mixtures

Mixture	C_{11}	C_{12}	C_f	S_f
M-B	3.59E-04	0.641	0.67	4.11E+04
M-NB	3.37E-04	0.640	0.55	7.69E+04
M-CB	5.10E-04	0.623	0.47	6.93E+04

The outcomes synthesized in Figure 3 and in Table 6 indicate that in comparison to the reference unmodified mixture, the asphalt mixtures containing nanoparticles were able to endure a higher damage until failure (S_f), ultimately reaching lower levels of material integrity (C_f).

It should be emphasized that the DCC should not be employed for the direct assessment of the fatigue life of asphalt mixtures. For such a purpose it is necessary to combine the DCC with a selected fatigue criterion. Thereafter, once the regression coefficients C_{11} and C_{12} are computed, the S-VECD model can be employed to simulate direct tension cyclic fatigue tests.[28,39] The number of loading cycles to failure can be predicted by combining Equation 11 with Equation 12 and by integrating the resulting expression as indicated in Equation 13:

$$\frac{dS}{dN} = \frac{dS\,d\xi}{d\xi\,dN} = \frac{dS}{d\xi}\left(\frac{1}{f_{red}}\right) = \left(-\frac{1}{2}\left(\varepsilon^{R}_{0,ta}\right)^{2}\frac{\partial C}{\partial S}\right)^{\alpha} K_1\left(\frac{1}{f_R}\right) \tag{11}$$

$$\frac{\partial C}{\partial S} = -\,C_{11}C_{12}S^{C_{12}-1} \tag{12}$$

$$\int_{S_{initial}}^{S_{failure}} \left(S^{(C_{12}-1)}\right)^{-\alpha} dS = \int_{1}^{N_{failure}} \left(\frac{1}{2}\left(\varepsilon^{R}_{0,ta}\right)^{2} C_{11}C_{12}\right)^{\alpha} K_1\left(\frac{1}{f_R}\right) dN \tag{13}$$

By assuming $S_{initial} >> S_{failure}$ and $N_{failure} >> 1$, the following expression is obtained (Equation 14):

$$\frac{S_f^{\alpha - \alpha C_{12} + 1}}{\alpha - \alpha C_{12} + 1} = \left(\frac{1}{2}\left(\varepsilon^{R}_{0,ta}\right)^{2} C_{11}C_{12}\right)^{\alpha} K_1\left(\frac{1}{f_R}\right)(N_f) \tag{14}$$

By considering the explicit formulation of the expression of the cyclic portion of pseudo strain (Equation 15), the predicted loading cycles to failure N_f can be finally calculated by means of Equation 16:

$$\left(\varepsilon^{R}{}_{0,ta}\right)_i = \frac{1}{E_R} \cdot \frac{\beta + 1}{2}\left[\left(\varepsilon_{0,pp}\right)_i \cdot \left|E^*\right|_{LVE}\right] \tag{15}$$

$$N_f = \frac{(f_R)(2^{3\alpha})S_f^{\alpha - \alpha C_{12} + 1}}{(\alpha - \alpha C_{12} + 1)(C_{11}C_{12})^{\alpha}\left[(\beta + 1)(\varepsilon_{0,pp})\left(\left|E^*\right|_{LVE}\right)\right]^{2\alpha} K_1} \tag{16}$$

where $\varepsilon_{0,pp}$ is the peak-to-peak strain; β is the load form factor; $|E^*|_{LVE}$ is the linear viscoelastic dynamic modulus; S_f is the cumulative damage at the failure point; K_1 is the loading shape factor; α is the damage evolution rate.

Results of fatigue test simulations carried out for the considered asphalt mixtures are shown in Figure 4. In order to more easily compare the three mixtures, Equation 16 can be simplified and rearranged as indicated in Equation 17:

$$N_f = k_1 \varepsilon_{0,pp}{}^{k_2} \tag{17}$$

where k_1 and k_2 are the parameters which are normally considered in the analysis of the results of fatigue tests plotted in the classical form of Whöler curves (Table 7).

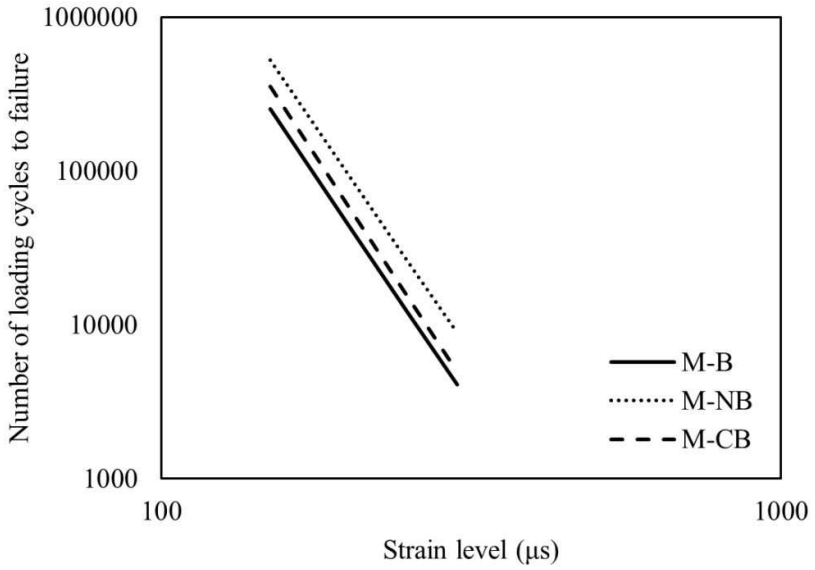

Fig. 4. Fatigue test simulation results for asphalt mixtures

Table 7. Fatigue parameters of asphalt mixtures

Mixture	k_1	k_2
M-B	2.223E+18	-5.949
M-NB	3.381E+18	-5.887
M-CB	8.868E+18	-6.158

Results shown in Figure 4 and in Table 7 clearly indicate that nano-modification of the bituminous binder led to a non-negligible enhancement of the fatigue performance of the reference asphalt mixture M-B. This can be explained by referring to the barrier effect played by the carbon nanotubes and organophilic nanoclay within the asphalt matrix, which may be able to hinder the evolution of microcracks through mechanisms that involve the formation of complex meshes and intercalated/exfoliated configurations, respectively.

As expected, the effectiveness of modification was found to be a function of the employed nano-additive. In the case of carbon nanotubes, the characteristic fatigue curve of the reference asphalt mixture was shifted upwards (i.e. with an increase of parameter k_1), with an increase of its slope (i.e. with an increase of k_2). This second

aspect suggests that an inversion of the relative ranking of the two mixtures (M-B and M-CB) may occur at very high strain levels, where the benefits associated to the presence of local entanglements and agglomerations may be lost. However, such a possibility would need to be checked by means of direct testing. When considering the effects of nanoclay modification, observed fatigue improvements were remarkably greater than those induced by carbon nanotubes. This can be clearly assessed by observing the relative position of the fatigue curves displayed in Figure 4, and by considering the fact that the k_2 parameter of mixture M-NB was almost identical to that to the reference mixture M-B. Thus, in this case the two fatigue lines are almost parallel and no inversion of the relative ranking of the mixtures is expected at very high strain levels. These outcomes suggest that the barrier effects created by nanoclay particles through the presence of intercalated/exfoliated configurations may be more effective than those associated to the dispersion in the bituminous matrix of carbon nanotubes.

Conclusions

Based on the results of experimental tests and simulations presented in this paper, it can be concluded that the use of nano-additives for the modification of bituminous binders can lead to a non-negligible enhancement of the fatigue damage resistance of asphalt mixtures. In particular, when considering an organophilic nanoclay and multiwall carbon nanotubes, improvements can be observed both by focusing on damage characteristic curves derived from viscoelastic continuum damage modelling and by considering the more classical Whöler curves. Observed effects are believed to be related to the interactions taking place between the nanoparticles and the bituminous binder, which can form, depending upon the case, different internal structures as a result of entanglement, agglomeration, intercalation and exfoliation phenomena. Experimental results also indicate that these interactions only marginally affect the linear viscoelastic properties of asphalt mixtures, in conditions which are far from damage.

Damage characteristic curves derived from cyclic direct tension fatigue tests showed that both nano-sized additives, when employed at their optimal dosage, improved the capability of the asphalt mixture to endure damage. Analysis of the Whöler curves highlighted the superior performance of the mixture containing organophilic nanoclay, in which the barrier effects created by intercalated or exfoliated configurations appeared to be more effective than those created by carbon nanotubes in counteracting crack initiation and in delaying crack propagation.

The results and conclusions outlined above refer to the specific nano-sized additives and asphalt mixtures which were considered in the described study. However, they may constitute a useful reference for the performance-related assessment and design of other similar additives and mixtures for which the same testing and modelling approach followed in this investigation can be employed for the identification and optimization of the effects produced by nano-modification.

References

1 Gopalakrishnan K, Birgisson B, Taylor P, Attoh-Okine NO, eds. Nanotechnology in Civil Infrastructure: A Paradigm Shift. Berlin Heidelberg: Springer-Verlag; 2011.

2 Li R, Xiao F, Amirkhanian S, You Z, Huang J. Developments of nano materials and technologies on asphalt materials – A review. *Constr Build Mater.* 2017;143: 633–648.

3 Yang J, Tighe S. A Review of Advances of Nanotechnology in Asphalt Mixtures. *Procedia - Soc Behav* Sci. 2013;96: 1269–1276.

4 Le Baron P. Polymer-layered silicate nanocomposites: an overview. *Appl Clay Sci.* 1999;15: 11–29.

5 Dai H. Carbon Nanotubes: Synthesis, Integration, and Properties. *Acc Chem Res*. 2002;35: 1035–1044.

6 Popov VN. Carbon nanotubes: properties and application. *Mater Sci Eng* R Rep. 2004;43: 61–102.

7 Pavlidou S, Papaspyrides CD. A review on polymer–layered silicate nanocomposites. *Prog Polym Sci*. 2008;33: 1119–1198.

8 Rahmat M, Hubert P. Carbon nanotube–polymer interactions in nanocomposites: A review. *Compos Sci Technol*. 2011;72: 72–84.

9 Ashish PK, Singh D, Bohm S. Evaluation of rutting, fatigue and moisture damage performance of nanoclay modified asphalt binder. *Constr Build Mater.* 2016;113: 341–350.

10 Santagata E, Baglieri O, Tsantilis L, Chiappinelli G. Effects of Nano-sized Additives on the High-Temperature Properties of Bituminous Binders: A Comparative Study. In: Kringos N, Birgisson B, Frost D, Wang L, eds. *Multi-Scale Modeling and Characterization of Infrastructure Materials*. Dordrecht: Springer Netherlands; 2013:297–309.

11 Santagata E, Baglieri O, Tsantilis L, Chiappinelli G. Fatigue and healing properties of nano-reinforced bituminous binders. *Int J Fatigue*. 2015;80: 30–39.

12 Santagata E, Baglieri O, Tsantilis L, Chiappinelli G. Fatigue properties of bituminous binders reinforced with carbon nanotubes. *Int J Pavement Eng*. 2015;16: 80–90.

13 Santagata E, Baglieri O, Tsantilis L, Chiappinelli G, Brignone Aimonetto I. Effect of sonication on high temperature properties of bituminous binders reinforced with nano-additives. *Constr Build Mater*. 2015;75: 395–403.

14 Santagata E, Baglieri O, Tsantilis L, Dalmazzo D, Chiappinelli G. Fatigue and healing properties of bituminous mastics reinforced with nano-sized additives. *Mech Time-Depend Mater*. 2016;20: 367–387.

15 Santagata E, Baglieri O, Tsantilis L, Dalmazzo D. Rheological Characterization of Bituminous Binders Modified with Carbon Nanotubes. *Procedia - Soc Behav Sci*. 2012;53: 546–555.

16 Santagata E, Baglieri O, Tsantilis L, Chiappinelli G, Dalmazzo D. Bituminous-based nanocomposites with improved high-temperature properties. *Compos Part B Eng*. 2016;99: 9–16.

17 You Z, Mills-Beale J, Foley JM, et al. Nanoclay-modified asphalt materials: Preparation and characterization. Constr Build Mater. 2011;25: 1072–1078.

18 Van de Ven, M.F.C., Molenaar, A.A.A., Besamusca J. Nanoclay for binder modification of asphalt mixtures. *Advan Test and Charact of B Mater.* 2015; Taylor & Francis Group, London, UK, 133-142.

19 Miglietta F, Underwood BS, Tsantilis L, Baglieri O, Kaloush KE, Santagata E. Fatigue properties of nano-reinforced bituminous mixtures: a viscoelastic continuum damage approach. *Int J Pavement Res Technol*. May 2018.

20 de Melo JVS, Trichês G. Evaluation of properties and fatigue life estimation of asphalt mixture modified by organophilic nanoclay. *Constr Build Mater*. 2017;140: 364–373.

21 Ameri M, Nowbakht S, Molayem M, Aliha MRM. Investigation of fatigue and fracture properties of asphalt mixtures modified with carbon nanotubes. *Fatigue Fract Eng Mater Struct*. 2016;39: 896–906.

22 Arabani M, Faramarzi M. Characterization of CNTs-modified HMA's mechanical properties. *Constr Build Mater*. 2015;83: 207–215.

23 de Melo JVS, Trichês G, de Rosso LT. Experimental evaluation of the influence of reinforcement with Multi-Walled Carbon Nanotubes (MWCNTs) on the properties and fatigue life of hot mix asphalt. *Constr Build Mater*. 2018;162: 369–382.

24 Santagata, E., Baglieri, O., Dalmazzo, D., & Tsantilis, L. Rheological and Chemical Investigation on the Damage and Healing Properties of Bituminous Binders. *J Assoc Asph Paving Technol*. 2009;78, pp. 567-596.

25 Santagata E, Baglieri O, Tsantilis L, Chiappinelli G. Storage Stability of Bituminous Binders Reinforced with Nano-Additives. In: Canestrari F, Partl MN, eds. 8th RILEM International Symposium on Testing and Characterization of Sustainable and Innovative Bituminous Materials. RILEM Bookseries. Springer Netherlands; 2016:75–87.

26 Chehab GR, Kim YR, Schapery RA, Witczak MW, Bonaquist R. Time-Temperature Superposition Principle For Asphalt Concrete With Growing Damage in Tension State. *Asph Paving Technol*. 2002;71: 559–593.

27 Cao W, Norouzi A, Kim YR. Application of viscoelastic continuum damage approach to predict fatigue performance of Binzhou perpetual pavements. *J Traffic Transp Eng Engl Ed*. 2016;3: 104–115.

28 Underwood BS, Baek C, Kim YR. Simplified Viscoelastic Continuum Damage Model as Platform for Asphalt Concrete Fatigue Analysis. *Transp Res Rec J Transp Res Board*. 2012;2296: 36–45.

29 Phan CV, Di Benedetto H, Sauzéat C, Dayde J, Pouget S. Quantification of different effects occurring during fatigue tests on bituminous mixtures. *Fatigue Fract Eng Mater Struct*. 2017;40: 2169–2182.

30 Daniel JS, Kim YR. Development of a Simplified Fatigue Test and Analysis Procedure Using a Viscoelastic, Continuum Damage Model. *J Assoc Asph Paving Technol*. 2002;71: 37.

31 Underwood BS, Kim YR, Guddati MN. Improved calculation method of damage parameter in viscoelastic continuum damage model. *Int J Pavement Eng*. 2010;11: 459–476.

32 Schapery RA. A theory of mechanical behavior of elastic media with growing damage and other changes in structure. *J Mech Phys Solids*. 1990;38: 215–253.

33 Underwood, B. S., Kim, Y.R., & Guddati, N.M. (2006). Characterization and performance prediction of ALF mixtures using a viscoelastoplastic continuum damage model, *J Assoc Asph Paving Technol*. 75 (2006), 577-636

34 Schapery RA. Correspondence principles and a generalizedJ integral for large deformation and fracture analysis of viscoelastic media. *Int J Fract*. 1984;25: 195–223.

35 Kim, Y. R., M. N. Guddati, B. S. Underwood, T. Y. Yun, V. Subramanian, S. Savadatti, and S. Thirunavukkarasu (2008). Development of a Multiaxial VEPCD-FEP++. Publication FHWA-HRT-08-073. FHWA, U.S. Department of Transportation.

36 Lee H-J, Daniel JS, Kim YR. Continuum Damage Mechanics-Based Fatigue Model of Asphalt Concrete. *J Mater Civ Eng*. 2000;12: 105–112.

37 Lee H-J, Kim YR. Viscoelastic Continuum Damage Model of Asphalt Concrete with Healing. *J Eng Mech*. 1998;124: 1224–1232.

38 Reese R. Properties of Aged Asphalt Binder Related to Asphalt Concrete Fatigue Life. *J Assoc Asph Paving Technol*. 1997;66: 604-632.

39 Hou, T., Underwood, B. S., & Kim, Y. R. Fatigue Performance Prediction of North Carolina Mixtures Using the Simplified Viscoelastic Continuum Damage Model. *J Assoc Asph Paving Technol.* 2010;79 pp. 35-73.